

MOL #109678

**Teaching an old drug new tricks: agonism, antagonism and biased signaling of
pilocarpine through M3 muscarinic acetylcholine receptor**

Alexey N. Pronin, Qiang Wang and Vladlen Z. Slepak

Department of Molecular and Cellular Pharmacology, University of Miami Miller School
of Medicine, Miami, FL 33136

MOL #109678

Running title:

Signaling bias and antagonism of pilocarpine for M3 receptor

Corresponding authors:

Vladlen Z. Slepak, Tel: (305)-243-3430; Fax: (305)-243-4555; vslepak@med.miami.edu.

Alexey N. Pronin, Tel: (305)-243-3431; Fax: (305) 243-4555;

a.pronin@med.miami.edu.

Number of text pages – 33

Number of tables – 1

Number of figures – 9

Number of references - 40

Number of words in the Abstract - 243

Number of words in the Introduction - 743

Number of words in the Discussion - 1494

Abbreviations: CCh - carbachol, DAG – diacylglycerol, ERK – extracellular regulated kinase, eYFP – enhanced yellow fluorescent protein, GPCR – G protein-coupled receptor, HBSS – Hank’s balanced salt solution, IP3 - inositol 1,4,5-trisphosphate, KRB – Krebs-Ringer bicarbonate buffer, M1R – M1 muscarinic receptor, M3R – M3 muscarinic receptor, Oxo – oxotremorine, Oxo-M - oxotremorine-M, PIP2 - phosphatidylinositol 4,5-bisphosphate, PKC – protein kinase C, PLC – phospholipase C, RFP – red fluorescent protein.

MOL #109678

ABSTRACT

Pilocarpine is a prototypical drug used to treat glaucoma and dry mouth and classified as either a full or partial muscarinic agonist. Here, we report several unexpected results pertaining to its interaction with muscarinic M3 receptor (M3R). We found that pilocarpine was 1,000 times less potent in stimulating mouse eye pupil constriction than muscarinic agonists oxotremorin-M (Oxo-M) or carbachol (CCh), even though all three ligands have similar K_d values for M3R. In contrast to CCh or Oxo-M, pilocarpine does not induce Ca^{2+} mobilization via endogenous M3R in HEK293T or mouse insulinoma MIN6 cells. Pilocarpine also fails to stimulate insulin secretion, and instead, antagonizes insulinotropic effect of Oxo-M and CCh-induced Ca^{2+} upregulation. However, in HEK293T or CHO-K1 cells overexpressing M3R, pilocarpine induces Ca^{2+} transients like those recorded with another Gq-coupled muscarinic receptor, M1R. Stimulation of cells overexpressing M1R or M3R with CCh resulted in a similar reduction in PIP2. In contrast to CCh, pilocarpine stimulated PIP2 hydrolysis only in cells overexpressing M1R, but not M3R. Moreover, pilocarpine blocked CCh-stimulated PIP2 hydrolysis in M3R-overexpressing cells, thus, it acted as an antagonist. Pilocarpine activates ERK1/2 in MIN6 cells. The stimulatory effect on ERK1/2 was blocked by the Src family kinase inhibitor PP2, indicating that the action of pilocarpine on endogenous M3R is biased toward β -arrestin. Taken together, our findings show that pilocarpine can act as either an agonist or antagonist of M3R, depending on the cell type, expression level and signaling pathway downstream of this receptor.

MOL #109678

Introduction.

Neurotransmitter acetylcholine plays a fundamental role in central and peripheral nervous systems. Receptors of acetylcholine and proteins involved in its synthesis, secretion and degradation are established targets for pharmacological intervention (reviews (Kruse et al., 2014b; Soukup et al., 2017; Wess, 2004)). Acetylcholine receptors that belong to the muscarinic class are G protein-coupled receptors (GPCRs), which are products of five genes (*Chrm1-5*). Muscarinic M1, M3 and M5 receptors are coupled to Gq and are known to mobilize free cytosolic Ca²⁺, whereas M2 and M4 receptors are coupled to Gi and down-regulate cAMP and regulate ion channels (Burford et al., 1995; Haga, 2013; Lechleiter et al., 1989).

M3 receptor (M3R) is interesting in several ways. It is highly expressed in certain areas of the nervous system and many endocrine and exocrine glands, playing a major role in hormone secretion (reviews: (Gautam et al., 2008; Kruse et al., 2014a)). For example, it is responsible for cholinergic stimulation of insulin release (Kong and Tobin, 2011; Ruiz de Azua et al., 2012). Other notable sites of M3R expression are the vascular endothelial cells and smooth muscle, such as the circular sphincter that closes the eye pupil (Bymaster et al., 2003). At the molecular level, M3R differs from other muscarinic receptors in that it has an unusually large (~24 kDa) 3rd intracellular loop, which interacts with many unique binding partners (Kan et al., 2014; Sandiford et al., 2010; Simon et al., 2006; Wu et al., 2000). Through stimulation of its cognate G protein, Gq, M3R activates the effector enzyme phospholipase C beta (PLC β), which hydrolyses

MOL #109678

phospholipid PIP₂, leading to generation of second messengers IP₃, DAG and Ca²⁺. Like many other GPCRs, M₃R can also activate protein kinases via β -arrestin and participates in unique interactions with several other proteins (Budd et al., 2000; Kan et al., 2014; Simon et al., 2006; Wu et al., 2000). Recently determined crystal structures of M₃R and other muscarinic receptors characterized molecular architecture of these GPCRs, providing valuable insights into organization of their orthosteric binding sites (Kruse et al., 2012; Thal et al., 2016).

The canonical paradigm in pharmacology postulates that an orthosteric ligand of a given receptor can be classified as a full or partial agonist, antagonist or inverse agonist and either activates or inhibits different signaling pathways mediated by the same receptor, to the same degree. In the past decade, this model has been rapidly evolving to accommodate the effects of many drugs that could not be described solely by these terms. It has been observed that, as a single receptor couples to different signal transduction pathways, the degree to which each pathway is activated depends on the nature of the ligand bound to the receptor. Such phenomena are now referred to as functional selectivity, biased signaling or biased agonism. One of the first observations was an early finding that an antagonist of cholecystokinin receptor D-Tyr-Gly-[(Nle_{28,31},D-Trp₃₀)cholecystokinin-26-32]-phenethyl ester induces internalization of the receptor (i.e., stimulates β -arrestin pathway) without activation of a G protein (Roettger et al., 1997). Another notable example is the stimulation of ERK activity via β -adrenergic receptors by such clinically important drugs as beta blockers propranolol and carvedilol (Azzi et al., 2003; Wisler et al., 2007). Since those early observations, biased signaling

MOL #109678

was reported for many receptors and ligands, thus becoming a general concept (Luttrell and Gesty-Palmer, 2010; Violin and Lefkowitz, 2007).

Pilocarpine is an alkaloid that has been used to treat glaucoma since 1875. Historical studies of its agonistic effect on salivary secretion and antagonism toward atropine led to development of the basic concept of a drug receptor ("receptive substance") in 1905 (Maehle, 2004). Since that time, numerous physiological and pharmacological studies established that pilocarpine selectively stimulates muscarinic receptors and has no nicotinic receptor action. Pilocarpine can activate all five muscarinic receptor subtypes, but most of the therapeutic effects of pilocarpine observed in humans are mediated by M3R. While there is a substantial number of publications describing effects of pilocarpine on M2R (*e.g.*, (Gregory et al., 2010), surprisingly few studies investigated its effects on M3R. Pilocarpine is generally classified as a full or partial agonist (Gurwitz et al., 1994; Karpinsky-Semper et al., 2014; Sykes et al., 2009). In this paper, we report previously unappreciated aspects of pilocarpine pharmacology as it relates to M3R. Whereas pilocarpine is a full agonist for M1R, we show that it can act as an antagonist for M3R under certain conditions. We also provide evidence for strong signaling bias of pilocarpine toward arrestin-Src pathway downstream of M3R.

MOL #109678

Materials and Methods

Reagents. Pilocarpine ((3S,4R)-3-Ethyl-4-((1-methyl-1H-imidazol-5-yl)methyl)dihydrofuran-2(3H)-one), carbachol (2-[(Aminocarbonyl)oxy]-N,N,N-trimethylethanaminium chloride), oxotremorine-M (oxotremorine methiodide, *N,N,N*-trimethyl-4-(2-oxo-1-pyrrolidinyl)-2-butyn-1-ammonium iodide), oxotremorine (1-(4-Pyrrolidin-1-ylbut-2-yn-1-yl)pyrrolidin-2-one), cevimeline ((2R,2'R)-2'-Methylspiro[4-azabicyclo[2.2.2]octane-2,5'-[1,3]oxathiolane]) and acetylcholine (2-Acetoxy-N,N,N-trimethylethanaminium) were purchased from Sigma-Aldrich (St. Louis, MO). PP2 (4-amino-5-(4-chlorophenyl)-7-(dimethylethyl)pyrazolo[3,4-d]pyrimidine) was from Abcam, bisindolylmaleimide I-HCl was from ChemCruz.

Hanks' balanced salt solution (HBSS) with or without Ca^{2+} and fura-2, AM were acquired from Life Technologies (Carlsbad, CA). The cDNA encoding human M1R and M3R in pcDNA3.1 were purchased from cDNA.org.

Mouse eye pupil constriction. All animal procedures were performed according to the Guidelines for the Care and Use of Laboratory Animals of the National Institutes of Health and protocols approved by the University of Miami Animal Use and Care Committee. Age-matched (12-18-week-old) C57Bl6/6J males were used for organ collection. The experiments were conducted at room temperature (20°C). Enucleated eyes were rinsed in HBSS and placed into a well of a custom designed Styrofoam rack filled with 100 μl HBSS. Before stimulating constriction, a picture of each eye was taken at the same magnification to record the open pupil diameter at time zero. Then 100 μl of either

MOL #109678

HBSS or a stimulant in HBSS (at 2x final concentration) were added and images were taken at the indicated time points. After the images were displayed on a computer monitor, pupil diameter at each time point was compared to the value at time zero (100%). Typically, the pupil of an enucleated eye remained wide open in the absence of a stimulus (pilocarpine or another agonist) for up to 90 minutes.

***In situ* RNA hybridization.** Localization of *Chrm3* messenger RNA was done using a custom fluorescence RNAscope probe (Advanced Cell Diagnostics). Experiments were performed with minor modifications of the manufacturer instructions, as described earlier (Pronin et al., 2014), using paraffin-embedded slices of the mouse eyes.

Free intracellular Ca²⁺ assays. HEK293T, CHO or MIN6 cells were grown on poly-L-lysine-coated 12-mm glass coverslips, washed with the culture medium and then incubated at 37°C in the culture medium containing 2 μM fura-2, AM for 60 minutes. After loading fura-2, AM, the cells were kept at ambient temperature for no longer than 1.5 hours before imaging. Coverslips were secured in a flow chamber and mounted on the stage of a Nikon TE2000 inverted fluorescence microscope. The cells were continuously superfused with HBSS by gravity flow. To stimulate the cells, the flow was switched to agonist-containing HBSS for a time required by a specified experiment, and then back to the agonist-free buffer. Images were collected in real time every 5 seconds using a 20× UV objective lens and recorded using MetaFluor software (Molecular Devices). The excitation wavelengths were 340 nm (Ca²⁺ bound) and 380 nm (Ca²⁺ free), with the emission set to 510 nm. The 340/380 ratio is representative of intracellular free [Ca²⁺].

MOL #109678

Individual cells or clusters of 10-20 cells were selected as regions of interest for signal quantification. Traces shown in the figures are averages of two to four independent experiments with three replicate coverslips per experiment.

Simultaneous calcium imaging recordings from cells transfected with two different

receptors. To simultaneously record Ca^{2+} responses from cells transfected with different sets of genes CHO or HEK293T cells were grown in 12-well plates to 70% confluency.

In one well the cells were co-transfected with plasmids containing eYFP and M1R using FuGENE 6 transfection reagent (Promega). In a separate well, the cells were co-

transfected with plasmids containing mCherry and M3R. The next day cells in both wells were trypsinized, mixed together and plated on poly-L-lysine-coated 12-mm glass

coverslips in 24-well plates. The day after, Ca^{2+} responses from cells were recorded as described above. In addition to fura-2 fluorescence, we recorded fluorescent signals from

eYFP (excitation 514 nm, emission 527 nm) and mCherry (excitation 587 nm, emission 610 nm). Individual green and red fluorescent cells were selected as regions of interest

for Ca^{2+} signal quantification. We also selected non-fluorescent cells as a control representing untransfected cells. Ca^{2+} responses from 30-40 cells of the same kind were

quantified and averaged.

Live PIP2 imaging. We used a protein sensor that increases its fluorescence upon

binding of PIP2 (Montana Molecular). It is a fusion between a dimerization-dependent

red fluorescent protein and the PH domain from PLC δ . CHO or HEK293T cells were co-transfected with a plasmid containing PIP2 sensor and a plasmid containing either M3R

MOL #109678

or M1R using FuGENE 6 transfection reagent. The next day cells were trypsinized and plated on poly-L-lysine-coated 12-mm glass coverslips. The day after, coverslips were secured in a flow chamber and mounted on the stage of a Nikon TE2000 inverted fluorescence microscope. The cells were continuously superfused by gravity flow with HBSS. To stimulate the cells, the flow was switched to agonist-containing HBSS for a specified time, and then changed back to the agonist-free buffer. Images were collected in real time every 5 seconds using a 20× objective lens and recorded using MetaFluor software (Molecular Devices). The excitation wavelength was 550 nm, with the emission set to 570 nm. Individual cells were selected as regions of interest for signal quantification. Traces shown here are averages of 10-20 cells from two to four independent experiments with three replicate coverslips per experiment. The peak response below the basal value was used for signal quantification.

MIN6 culture, stimulation and insulin ELISA. Cells were cultured in DMEM (Invitrogen, USA) with 25 mM glucose and 4 mM L-glutamine supplemented with 10% FBS, 100 µg/ml penicillin/100 µg/ml streptomycin, 50 µM β-mercaptoethanol, 1 mM sodium pyruvate and 10 mM HEPES pH 7.2. For a typical test, cells were suspended in DMEM, seeded at 3×10^5 per well in 24-well plates and grown to 80% confluency. Prior to application of stimulants, cells were pre-incubated with serum- and glucose-free DMEM for 1 h, then washed twice with KRB buffer containing 0.1% BSA, after which various agents required by the experiment were added in KRB. The supernatant from the stimulated cells was collected after 30 min at 37°C and stored frozen at -80°C until measurement of insulin. Samples were analyzed using mouse insulin “sandwich” ELISA

MOL #109678

kit (Merckodia, Sweden) per the manufacturer's protocol and using sample dilutions to ensure that the signal was within the linear range of sensitivity.

ERK1/2 phosphorylation assay. MIN6 cells were grown in 12-well plates to 40% confluency. Prior to stimulation with muscarinic agonists they were serum-starved for 4 h. If a protein kinase inhibitor (PP2 and bisindolylmaleimide I) was used in an experiment, it was included in the serum starvation medium. The cells were stimulated for 5 min, the culture medium was quickly aspirated and the cells were harvested by the addition of 160 μ l of 1x SDS PAGE Sample Buffer. Cell lysates were briefly sonicated to destroy chromosomal DNA and resolved on SDS-polyacrylamide gels, followed by immunoblotting using antibodies against P-ERK1/2 (T202/Y204) (rabbit polyclonal, Cell Signaling Technology) and actin (mouse monoclonal, Millipore). The secondary antibodies labeled with infrared IRDye 800CW or 680RD were from LI-COR, Inc. The immune complexes were visualized using Odyssey (LI-COR) infrared fluorescence detection system. For quantitative analysis, the signal in the band of interest (*i.e.*, P-ERK) was normalized to the signal for actin in the same lane on the immunoblot.

Statistics. Data are reported as means \pm SD. GraphPad Prism software (version 6.07; GraphPad Software, La Jolla, CA) was used for statistical analysis. The EC₅₀ values were determined using nonlinear regression with a four-parameter logistic equation. Groups of data were compared using ANOVA or two-tailed unpaired Student's t-tests, with values of $P < 0.05$ considered statistically significant.

MOL #109678

Results

Effect of pilocarpine on pupil constriction. As expected, application of pilocarpine caused constriction of the mouse eye pupil (miosis), and its full effect was comparable to that of another cholinergic agonist, CCh (Fig. 1A, B). However, the estimated EC_{50} of pilocarpine is about 1,000 times higher than the EC_{50} determined under the same conditions for other cholinergic agonists, CCh or Oxo-M. Furthermore, the EC_{50} of pilocarpine is by three orders of magnitude higher compared to its reported K_d for M3R (30 μ M) (Sykes et al., 2009) (Fig. 1C). M3R was previously shown to be the only acetylcholine receptor mediating constriction of the sphincter muscle by demonstrating lack of miosis in the *Chrm3* knockout mice (Bymaster et al., 2003). Here we confirm that the *Chrm3* gene is expressed in the sphincter muscle by RNA *in situ* hybridization (Fig. 1D). To explain the relatively low potency of pilocarpine compared to other agonists, we hypothesized that it activates different signal transduction pathways and set out to investigate its ability to stimulate canonical intracellular signals in cell models.

Pilocarpine antagonizes CCh-induced Ca^{2+} mobilization in HEK293T cells.

To test signaling mechanisms downstream of M3R we first turned to HEK293T cells, a system that is more amenable to analysis of second messengers than the sphincter pupillae muscle. Previous studies showed that HEK293T cells only express M3 (not M1) receptor, and cholinergic agonists cause upregulation of Ca^{2+} via the canonical Gq-mediated pathway (Atwood et al., 2011; Luo et al., 2008). Accordingly, we detected robust increases in free Ca^{2+} concentration upon application of CCh, with an EC_{50} of 11 ± 2

MOL #109678

μM (Fig. 2A, B). However, under the same conditions, pilocarpine fails to elicit any Ca^{2+} response at concentrations up to 1 mM. To test if pilocarpine actually interacted with the receptor, we applied it together with CCh and found that pilocarpine completely blocked the CCh-induced signal (Fig. 2B). Thus, we came to an unexpected conclusion that pilocarpine functions as an M3R antagonist by competitively inhibiting CCh-stimulated rise in cytoplasmic free Ca^{2+} .

Next, to investigate if the apparent pilocarpine antagonism can be observed in an alternative system naturally expressing M3R, we examined mouse insulinoma MIN6 cells. The MIN6 cell line is commonly used as a model for studying pancreatic beta cell biology and known to secrete insulin in response to cholinergic stimulation (Selway et al., 2012; Weng et al., 1993). As expected, application of Oxo-M resulted in a robust increase in free Ca^{2+} (Fig. 2C) and the amount of insulin released to the medium (Fig. 2D). In contrast, pilocarpine failed to induce Ca^{2+} response or insulin secretion. Moreover, pilocarpine inhibited insulinotropic effect of Oxo-M (Fig. 2D). Thus, pilocarpine acts as an M3R antagonist in MIN6 cells, similarly to its effect in HEK293T cells.

The antagonistic effect of pilocarpine toward M3R (Fig. 2) is surprising because this drug has been studied for decades both *in vivo* and *in vitro* and has been classified as an agonist. *In vivo*, the agonistic action of pilocarpine could be, in principle, explained by its effect on a different muscarinic receptor(s) along with M3R. However, numerous experiments with cells that do not have endogenous acetylcholine receptors show that,

MOL #109678

after overexpression of M3R, pilocarpine acts as an agonist (Karpinsky-Semper et al., 2014; Sykes et al., 2009). We therefore re-examined the behavior of M3R transfected into CHO-K1 cells, which do not express any muscarinic receptors. In these experiments, we compared M3R to M1R, another Gq-coupled muscarinic receptor known to be activated by the same agonists.

Pilocarpine stimulates Ca²⁺ mobilization via overexpressed M3R. In CHO-K1 cells transiently transfected with M3R, pilocarpine stimulated free Ca²⁺ increases that appeared to be as robust as Ca²⁺ transients recorded with transfected M1R (Fig. 3). To quantitatively compare signaling elicited by the two receptors we sought to minimize the assay variability between the M1R- and M3R-transfected cell preparations. For this purpose, we developed a system that allowed us to monitor M1R- and M3R-expressing cells simultaneously on the same glass slide. We co-transfected one batch of CHO-K1 cells with M1R together with a plasmid harboring fluorescent marker eYFP and another batch with M3R together with a different fluorescent marker, mCherry. After transfection, these two cell pools were lifted from the plates, mixed and re-plated onto coverslips, so that the "green" and "red" cells could be identified and analyzed within the same visual field (Fig. 3A-C). Our data show that CCh- or pilocarpine-induced Ca²⁺ responses of M3R and M1R-expressing cells were indistinguishable. The EC₅₀ of CCh was only ~3-fold lower than EC₅₀ of pilocarpine for both M1R and M3R, and there was no significant difference in potency of pilocarpine for M1R *versus* M3R (Fig. 3D, E). As expected, untransfected CHO-K1 cells, which had neither red nor green fluorescence and were always present in the preparations, showed no response to cholinergic stimulation.

MOL #109678

We performed similar transfection experiments on HEK293T cells, and found that pilocarpine caused Ca^{2+} signaling via overexpressed M3R (Fig. 3F). The untransfected HEK293T cells present in the same experiment only responded to CCh and not to pilocarpine.

These results show that – consistent with previous studies (Karpinsky-Semper et al., 2014; Sykes et al., 2009) – pilocarpine acts as a full agonist for overexpressed M3R. However, for endogenous M3R in HEK293T or MIN6 cells it acts as an antagonist.

Pilocarpine can stimulate M3R-mediated Ca^{2+} mobilization, but not PIP2 hydrolysis.

The variability in the effect of pilocarpine on free cytoplasmic Ca^{2+} in different experimental systems can be explained by activation of distinct pathways. To study signaling downstream of M3R but upstream of Ca^{2+} release we measured hydrolysis of the signaling lipid phosphatidylinositol 4,5-bisphosphate (PIP2). For this purpose, we employed a novel fluorescent biosensor that consists of mutated dimerization-dependent RFP fused to the PH domain of PLC δ . Upon binding to PIP2 this molecule increases fluorescence intensity (Tewson et al., 2012; Tewson et al., 2016; Tewson et al., 2013). Application of CCh on HEK293T cells co-transfected with the PIP2 sensor and M3R resulted in a notable drop in RFP fluorescence, evidently because of the increase in PIP2 hydrolysis by the M3R-stimulated PLC. In contrast to CCh, pilocarpine did not cause any detectable fluorescence change (Fig. 4A, B). In cells overexpressing M1R, both CCh and pilocarpine robustly reduced the PIP2 signal (Fig. 4B). Similarly, in transfected CHO-K1 cells, agonists CCh and Oxo-M stimulated PIP2 hydrolysis in the cells transfected with either M3R or M1R. Pilocarpine, however, was active only in cells

MOL #109678

expressing M1R, whereas no effect on PIP2 in M3R-expressing cells was detected (Fig. 4C). Furthermore, pilocarpine blocked CCh-stimulated PIP2 hydrolysis in M3R-overexpressing cells (Fig. 4D). Since either an antagonist or partial agonist can occupy the orthosteric site of a GPCR, they would displace a full agonist and inhibit the functional response. In our experiments, pilocarpine reduced PIP2 hydrolysis below the detection level; in fact, its effect was indistinguishable from that of atropine (data not shown). Therefore, in the M3R-stimulated breakdown of PIP2 assay pilocarpine acts as an antagonist rather than a partial agonist. On the other hand, the increase in intracellular Ca^{2+} was still observed when pilocarpine was added together with CCh (Fig. 4E), showing that in this assay pilocarpine acts as an agonist.

Taken together, our findings indicate that for M3R, pilocarpine can behave as either agonist or antagonist, depending on the expression level of the receptor and the downstream signaling. For M1R, pilocarpine is a full agonist regardless of the functional read-out.

To further investigate the relationship between PIP2 hydrolysis and Ca^{2+} mobilization, we examined the effects of pilocarpine and CCh on M3R and M1R overexpressed in CHO-K1 cells under the same conditions (Fig. 5A, B, Table 1). Our results with overexpressed M1R show that the EC_{50} in the Ca^{2+} assay was about 10-fold lower than the EC_{50} determined in the PIP2 assay for both CCh and pilocarpine. Thus, Ca^{2+} assay is significantly more sensitive to agonists compared to PIP2 assay. For example, at 0.2 μ M of either CCh or pilocarpine, PIP2 response is barely detectable (<10% of maximal), while Ca^{2+} increase is already at 40-80% of the maximum (Fig. 5A,

MOL #109678

the vertical green line). These results are consistent with earlier work (*e.g.*, (Evans et al., 1985) reporting higher potency of muscarinic agonists in stimulating Ca^{2+} *versus* PIP2 responses. The Ca^{2+} assay can be expected to be more sensitive than PIP2 hydrolysis because of signal amplification in the cascade where a relatively small number of IP3 molecules can trigger the release of numerous Ca^{2+} ions from the stores.

For M3R, the difference between the Ca^{2+} and PIP2 assays is more pronounced than for M1R. The EC_{50} determined for CCh in the Ca^{2+} assay with overexpressed M3R was about 70-fold lower than the EC_{50} value obtained in the PIP2 assay. The most striking difference is the complete inability of pilocarpine to induce PIP2 hydrolysis. Even if the concentration of pilocarpine was 1000 times higher than that required for saturation of the Ca^{2+} response, no change in PIP2 level was detected. These results lead us to conclude that stimulation of M3R with pilocarpine does not cause PIP2 hydrolysis and, presumably, IP3 production. To test if the increase in cytosolic free Ca^{2+} occurs through the influx of extracellular Ca^{2+} , we stimulated CHO-K1 cells overexpressing M3R in the absence of Ca^{2+} in the culture medium. There was still a robust Ca^{2+} response to pilocarpine (Fig. 5C) under these conditions, demonstrating that Ca^{2+} is released from an intracellular source(s).

Because of the differences in behavior of endogenous M3R *vs* overexpressed in CHO-K1 cells (Figs 2-5), we also used the free Ca^{2+} and PIP2 assays to compare the effect of CCh on endogenous *vs* overexpressed M3R in in the same cell line, HEK293T (Fig 6, Table 1). As one could expect, Ca^{2+} responses were much stronger with the

MOL #109678

transfected M3R: the determined EC_{50} for CCh was more than 250 times lower and the E_{max} was more than 2 times higher than with the endogenous receptor. Similar to CHO-K1 cells, the EC_{50} measured in the Ca^{2+} assay with overexpressed M3R was about 100 times lower than with PIP2 hydrolysis. As a result, at 0.2 μ M of CCh the PIP2 response is barely detectable (<5% of maximal), while Ca^{2+} increase is already at 80% of the maximum (Fig. 6, the vertical green line). The most striking result is that even though CCh induces Ca^{2+} responses via the endogenous receptor ($EC_{50}=11\pm2$ μ M), we were unable to detect any PIP2 hydrolysis even at millimolar concentration of CCh. This is consistent with an early finding that pilocarpine upregulated Ca^{2+} , but did not measurably increase inositol-phosphate accumulation in 1321N1 astrocytoma cells (Evans et al., 1985). A likely explanation is that at the endogenous level of M3R expression even high doses of agonist cause hydrolysis of only a small fraction of PIP2; this fraction is sufficient to stimulate the Ca^{2+} release, but is too low to be detected using either radioactively labeled PIP2 precursor or the fluorescent PIP2 biosensor.

To test if the inability to stimulate PIP2 hydrolysis via overexpressed M3R was unique to pilocarpine, we performed pilot experiments with two other muscarinic agonists, oxotremorine (Oxo) and cevimeline. Like pilocarpine, they stimulated Ca^{2+} responses (data not shown) and, similar to pilocarpine, neither Oxo nor cevimeline induced notable reduction in PIP2 (Fig. 7A). Under identical conditions, Oxo-M, CCh and acetylcholine stimulated robust PIP2 hydrolysis. One obvious common feature in the latter three agonists is the quaternary amine of the choline moiety (Fig. 7B). We speculate that this amine is the pharmacophore determining the ability of the drug to

MOL #109678

stabilize the conformation of overexpressed M3R in which it can activate both Ca^{2+} mobilization and PIP2 hydrolysis.

Pilocarpine stimulates ERK phosphorylation in MIN6 cells with a bias toward the Src-mediated pathway. Like other GPCRs, M3R is known to activate extracellular signal-regulated kinases, ERK1/2 (Guerra et al., 2014; Luo et al., 2008; Selway et al., 2012). Activation of ERK can occur via distinct mechanisms that can involve G protein- and β -arrestin-mediated pathways and result in ERK phosphorylation. We found that, like other muscarinic agonists, pilocarpine causes ERK1/2 phosphorylation in MIN6 cells (Fig. 8A, B). However, the EC_{50} for pilocarpine was about 10 times higher than that induced by Oxo-M, while the maximal level of pilocarpine-induced phosphorylation was only about 32% of that induced by Oxo-M. Since there is more than one signaling pathway that can couple M3R to ERK1/2 activation, we hypothesized that pilocarpine-bound M3R could activate only one of these mechanisms, for example, β -arrestin-mediated activation of Src kinase. We tested this idea by applying inhibitor of Src family kinases, 4-amino-5-(4-chlorophenyl)-7-(dimethylethyl)pyrazolo[3,4-*d*]pyrimidine known as PP2 (Fig. 8C) and found that it almost completely eliminated pilocarpine-induced ERK1/2 phosphorylation. In contrast, when MIN6 cells were stimulated with Oxo-M, more than 55% of ERK1/2 phosphorylation occurred even in the presence of the saturating (60 μM) concentration of PP2. This remaining ERK1/2 phosphorylation was almost completely blocked when an inhibitor of PKC (bisindolylmaleimide I, BIM) was included in the mix (Fig. 8D). These results are consistent with the model (Fig. 9) that in

MOL #109678

MIN6 cells pilocarpine acts on M3R as a partial agonist that is biased toward a pathway sensitive to PP2, likely the β -arrestin-Src pathway.

Discussion.

Pilocarpine is a prototypical cholinergic drug present on the World Health Organization List of Essential Medicines. Its ability to activate secretion by exocrine glands has been utilized for many decades to treat dry mouth and dry eye syndromes. Because it constricts smooth muscles in the eye releasing intraocular pressure, topical pilocarpine has been the treatment of choice for glaucoma. Early physiological experiments on pilocarpine-atropine competition led to the development of one of the most important biochemical and pharmacological concepts, the concept of a drug receptor. Our paper reveals previously unappreciated aspects of pilocarpine pharmacology by showing that its effect on M3R cannot be described solely by full or partial agonism. According to our data, pilocarpine can also act as an antagonist or biased agonist for this muscarinic receptor depending on cellular environment and the read-out used to study molecular events downstream of M3R stimulation.

Importantly, we compared our M3R data with a similar Gq-coupled muscarinic receptor, M1R. Our results on M1R are consistent with the common knowledge that pilocarpine is a full muscarinic agonist. It is worth noting the multiplex technique that we developed to compare the two receptors. The M1R- and M3R-expressing cells were marked by co-transfection with red and green fluorescent proteins, which allowed us to

MOL #109678

examine the two cell populations simultaneously under identical conditions in real time (Fig. 3). We recommend this simple method for comparing other receptors as well, particularly when the expected differences in the downstream signaling are small. For example, one could evaluate effects of drugs on closely related receptors, examine receptor mutants or the effects of co-expressed regulatory proteins.

In the Ca^{2+} mobilization assay, we did not detect a significant difference between the responses of overexpressed M1R and M3R to either CCh or pilocarpine (Fig. 4, Table 1). However, when we analyzed PIP2 hydrolysis in the same system, the difference between M1R and M3R was remarkable. For M1R, both CCh and pilocarpine acted as full agonists, eliciting a robust reduction in PIP2 level. M3R was also fully activated by CCh, but with pilocarpine we did not detect any change in PIP2 signal (Fig. 4, 5). Thus, pilocarpine is strikingly selective for pathways downstream of M3R. For the free Ca^{2+} increase it works as a full agonist. For PIP2 hydrolysis it does not elicit any response by itself and completely blocks the stimulatory effect of CCh. This apparent antagonism is unique for M3R-stimulated PIP2 hydrolysis. For other receptors and read-outs, pilocarpine works as a partial agonist with considerable efficacy, *e.g.*, it can stimulate M2R to about 70% of the maximal effect of CCh (Gregory et al., 2010). Our initial survey of cholinergic agonists shows that cevimeline and oxotremorine also fail to stimulate PIP2 hydrolysis via overexpressed M3R. We speculate that the quaternary amine absent in these compounds but present in acetylcholine, Oxo-M and CCh, is responsible for stimulation of Gq and PIP2 hydrolysis.

Another important finding of our study is the very different effect of pilocarpine on overexpressed *versus* endogenous M3R. We analyzed M3R function in three

MOL #109678

biological systems where it is known to be the sole muscarinic receptor: HEK293T cells, MIN6 cells and the constrictor muscle of the pupil. Surprisingly, pilocarpine did not stimulate Ca^{2+} mobilization in HEK293T or MIN6 cells at all (Fig. 2), unless M3R was overexpressed. Thus, pilocarpine-induced Ca^{2+} response in M3R-transfected cells can be interpreted as an artifact of the abnormally high receptor level. This notion is likely to have implication for other GPCRs, as transfected cells are widely used for receptor deorphanization, drug screening and delineation of signaling and regulatory mechanisms. Our results show that even for such a well-known pharmaceutical as pilocarpine, the answer to the basic question of whether it is an agonist or antagonist could be different for the native versus the overexpressed form of the same receptor. Clearly, drugs and receptors that have been investigated less than pilocarpine and the muscarinic family must be analyzed in the native context.

Pilocarpine also failed to stimulate insulin secretion in MIN6 cells and blocked insulin responses elicited by Oxo-M, and so it works as an M3R antagonist in the pancreatic beta cell model. On the other hand, pilocarpine stimulates pupil constriction, and even though it is much less potent than other agonists, it is a full agonist in this system. It has an unusually high EC_{50} that is three orders of magnitude above the reported K_d of pilocarpine for M3R. Accordingly, the concentration of pilocarpine in eye drops is extremely high – 2-4% (80-160 mM), and there is no explanation why the therapeutic dose is that high. Abnormally low ability of pilocarpine to cause activation of Gq was noticed earlier, when it was shown that pilocarpine-stimulated GTP γ S binding in M3R-transfected cells was several fold lower than with other agonists (Sykes et al., 2009). Data on pilocarpine-stimulated generation of IP3 is controversial: some investigators

MOL #109678

reported robust overexpressed M3R-mediated production (Ehlert et al., 1999), others found pilocarpine to be a virtually ineffective stimulant of the overexpressed or endogenous M3R (Evans et al., 1985; Gurwitz et al., 1994).

Together with the earlier observations, our results show that pilocarpine does not activate all signaling pathways triggered by M3R, which led us to propose that, unlike CCh and Oxo-M, pilocarpine can act as a biased agonist (Fig. 9). The following data in HEK293T and MIN6 cells support this model: pilocarpine does not activate Ca^{2+} via the endogenous M3R present in these cells, but does stimulate ERK, evidently via the β -arrestin-Src kinase mechanism. For ERK activation, pilocarpine fits under the definition of a partial agonist since the maximal level of ERK phosphorylation in the presence of pilocarpine is about three times less than that reached with Oxo-M. For the G protein pathway, application of pilocarpine causes inhibition of signaling induced by other agonists down to the basal level (Fig. 2), and, thus, it acts as an antagonist.

The model presented in Figure 9 can explain much of our current data and possibly earlier observations (Gurwitz et al., 1994; Sykes et al., 2009). However, our study also exposed some phenomena where the underlying mechanisms are unclear. For example, it is puzzling why in the basic assay of pupil constriction pilocarpine works as a full agonist but requires an extremely high concentration. Classic pharmacology cannot explain the observed difference in the effects of 1 mM (30-fold above the K_d , ~99% receptor occupancy) and 10 mM (300-fold above the K_d , ~99.9% receptor occupancy) pilocarpine. One hypothesis explaining why pilocarpine can act both as an agonist and antagonist toward M3R is the existence of two binding sites. The high affinity site would be the orthosteric site where it competes with CCh but does not activate Gq, *i.e.*, works as

MOL #109678

an antagonist. At the second, low affinity site, pilocarpine could additionally change the receptor conformation, switching it to the active form. The second pilocarpine molecule could occupy the outside vestibule area revealed by the M3R crystal structure (Kruse et al., 2012). However, the two binding sites model does not explain why even the millimolar concentrations of pilocarpine elicit no detectable Ca^{2+} responses via endogenous M3R in HEK293T cells (Fig 2).

Another observation that we cannot yet explain is how pilocarpine can increase Ca^{2+} via overexpressed M3R without inducing detectable PIP2 hydrolysis. In theory, Ca^{2+} can come from a source that does not require IP3, but instead is activated, for example, by phosphorylation initiated by β -arrestin or another mechanism downstream of M3R. Thus far, we found that in the absence of extracellular Ca^{2+} pilocarpine can still induce Ca^{2+} transients in CHO-K1 cells overexpressing M3R (Fig. 5C), which points to an intracellular Ca^{2+} source such as mitochondria. However, at the moment we favor a simpler explanation that is based on the assumption that very little IP3 is sufficient to trigger a full Ca^{2+} release from the endoplasmic reticulum. Indeed, there is a significant (1-2 orders of magnitude) shift to the right in the PIP2 compared to Ca^{2+} dose-response curves measured with overexpressed M3 even with CCh (Fig. 5B); it is possible that for pilocarpine this difference is even bigger. This hypothesis suggests that some IP3 is generated locally, whereas the biosensor assay we use in this study can only detect changes in global PIP2. Imaging techniques such as TIRF (Wuttke et al., 2016) and a knockdown of potentially relevant signaling components can test these ideas in the future.

Our current work showed for the first time that pilocarpine acts on M3R not only as a full or partial agonist as it is known to act on other muscarinic receptors, but also as

MOL #109678

an antagonist, and a functionally selective ligand. Since these behaviors are particularly apparent with the endogenous M3R, we speculate that these properties might explain why pilocarpine has fewer side effects than CCh when used to treat dry mouth or glaucoma. Understanding the structure-activity relationship in cholinergic drugs and receptors may expand their use for other diseases, such as diabetes, where biased signaling via M3R can improve the function and viability of beta cells.

Acknowledgements:

We would like to thank Dr. Daniel Isom for careful reading of the manuscript and excellent suggestions.

Authorship contributions:

Participated in research design: Pronin, Slepak.

Conducted experiments: Pronin, Wang.

Performed data analysis: Pronin, Wang, Slepak.

Wrote or contributed to the writing of the manuscript: Pronin, Slepak.

References

- Atwood BK, Lopez J, Wager-Miller J, Mackie K and Straiker A (2011) Expression of G protein-coupled receptors and related proteins in HEK293, AtT20, BV2, and N18 cell lines as revealed by microarray analysis. *BMC Genomics* **12**: 14.
- Azzi M, Charest PG, Angers S, Rousseau G, Kohout T, Bouvier M and Pineyro G (2003) Beta-arrestin-mediated activation of MAPK by inverse agonists reveals distinct active conformations for G protein-coupled receptors. *Proc Natl Acad Sci U S A* **100**(20): 11406-11411.
- Budd DC, McDonald JE and Tobin AB (2000) Phosphorylation and regulation of a Gq/11-coupled receptor by casein kinase 1alpha. *J Biol Chem* **275**(26): 19667-19675.
- Burford NT, Tobin AB and Nahorski SR (1995) Differential coupling of m1, m2 and m3 muscarinic receptor subtypes to inositol 1,4,5-trisphosphate and adenosine 3',5'-cyclic monophosphate accumulation in Chinese hamster ovary cells. *J Pharmacol Exp Ther* **274**(1): 134-142.
- Bymaster FP, Carter PA, Yamada M, Gomeza J, Wess J, Hamilton SE, Nathanson NM, McKinzie DL and Felder CC (2003) Role of specific muscarinic receptor subtypes in cholinergic parasympathomimetic responses, in vivo phosphoinositide hydrolysis, and pilocarpine-induced seizure activity. *Eur J Neurosci* **17**(7): 1403-1410.
- Ehlert FJ, Griffin MT, Sawyer GW and Bailon R (1999) A simple method for estimation of agonist activity at receptor subtypes: comparison of native and cloned M3 muscarinic receptors in guinea pig ileum and transfected cells. *J Pharmacol Exp Ther* **289**(2): 981-992.
- Evans T, Hepler JR, Masters SB, Brown JH and Harden TK (1985) Guanine nucleotide regulation of agonist binding to muscarinic cholinergic receptors.

MOL #109678

Relation to efficacy of agonists for stimulation of phosphoinositide breakdown and Ca²⁺ mobilization. *Biochem J* **232**(3): 751-757.

Gautam D, Jeon J, Li JH, Han SJ, Hamdan FF, Cui Y, Lu H, Deng C, Gavrilova O and Wess J (2008) Metabolic roles of the M3 muscarinic acetylcholine receptor studied with M3 receptor mutant mice: a review. *J Recept Signal Transduct Res* **28**(1-2): 93-108.

Gregory KJ, Hall NE, Tobin AB, Sexton PM and Christopoulos A (2010) Identification of orthosteric and allosteric site mutations in M2 muscarinic acetylcholine receptors that contribute to ligand-selective signaling bias. *J Biol Chem* **285**(10): 7459-7474.

Guerra ML, Wauson EM, McGlynn K and Cobb MH (2014) Muscarinic control of MIN6 pancreatic beta cells is enhanced by impaired amino acid signaling. *J Biol Chem* **289**(20): 14370-14379.

Gurwitz D, Haring R, Heldman E, Fraser CM, Manor D and Fisher A (1994) Discrete activation of transduction pathways associated with acetylcholine m1 receptor by several muscarinic ligands. *Eur J Pharmacol* **267**(1): 21-31.

Haga T (2013) Molecular properties of muscarinic acetylcholine receptors. *Proc Jpn Acad Ser B Phys Biol Sci* **89**(6): 226-256.

Kan W, Adjobo-Hermans M, Burroughs M, Faibis G, Malik S, Tall GG and Smrcka AV (2014) M3 muscarinic receptor interaction with phospholipase C beta3 determines its signaling efficiency. *J Biol Chem* **289**(16): 11206-11218.

Karpinsky-Semper D, Volmar CH, Brothers SP and Slepak VZ (2014) Differential effects of the Gbeta5-RGS7 complex on muscarinic M3 receptor-induced Ca²⁺ influx and release. *Mol Pharmacol* **85**(5): 758-768.

Kong KC and Tobin AB (2011) The role of M(3)-muscarinic receptor signaling in insulin secretion. *Commun Integr Biol* **4**(4): 489-491.

MOL #109678

Kruse AC, Hu J, Kobilka BK and Wess J (2014a) Muscarinic acetylcholine receptor X-ray structures: potential implications for drug development. *Curr Opin Pharmacol* **16**: 24-30.

Kruse AC, Hu J, Pan AC, Arlow DH, Rosenbaum DM, Rosemond E, Green HF, Liu T, Chae PS, Dror RO, Shaw DE, Weis WI, Wess J and Kobilka BK (2012) Structure and dynamics of the M3 muscarinic acetylcholine receptor. *Nature* **482**(7386): 552-556.

Kruse AC, Kobilka BK, Gautam D, Sexton PM, Christopoulos A and Wess J (2014b) Muscarinic acetylcholine receptors: novel opportunities for drug development. *Nat Rev Drug Discov* **13**(7): 549-560.

Lechleiter J, Peralta E and Clapham D (1989) Diverse functions of muscarinic acetylcholine receptor subtypes. *Trends Pharmacol Sci Suppl*: 34-38.

Luo J, Busillo JM and Benovic JL (2008) M3 muscarinic acetylcholine receptor-mediated signaling is regulated by distinct mechanisms. *Mol Pharmacol* **74**(2): 338-347.

Luttrell LM and Gesty-Palmer D (2010) Beyond desensitization: physiological relevance of arrestin-dependent signaling. *Pharmacol Rev* **62**(2): 305-330.

Maehle AH (2004) "Receptive substances": John Newport Langley (1852-1925) and his path to a receptor theory of drug action. *Med Hist* **48**(2): 153-174.

Pronin AN, Levay K, Velmeshev D, Faghihi MA, Shestopalov VI and Slepak VZ (2014) Expression of Olfactory Signaling Genes in the Eye. *PLoS One* DOI: **10.1371/journal.pone.0096435**.

Roettger BF, Ghanekar D, Rao R, Toledo C, Yingling J, Pinon D and Miller LJ (1997) Antagonist-stimulated internalization of the G protein-coupled cholecystokinin receptor. *Mol Pharmacol* **51**(3): 357-362.

MOL #109678

Ruiz de Azua I, Gautam D, Jain S, Guettier JM and Wess J (2012) Critical metabolic roles of beta-cell M3 muscarinic acetylcholine receptors. *Life Sci* **91**(21-22): 986-991.

Sandiford SL, Wang Q, Levay K, Buchwald P and Slepak VZ (2010) Molecular organization of the complex between the muscarinic M3 receptor and the regulator of G protein signaling, Gbeta(5)-RGS7. *Biochemistry* **49**(24): 4998-5006.

Selway JL, Moore CE, Mistry R, John Challiss RA and Herbert TP (2012) Molecular mechanisms of muscarinic acetylcholine receptor-stimulated increase in cytosolic free Ca(2+) concentration and ERK1/2 activation in the MIN6 pancreatic beta-cell line. *Acta Diabetol* **49**(4): 277-289.

Simon V, Guidry J, Gettys TW, Tobin AB and Lanier SM (2006) The proto-oncogene SET interacts with muscarinic receptors and attenuates receptor signaling. *J Biol Chem* **281**(52): 40310-40320.

Soukup O, Winder M, Killi UK, Wsol V, Jun D, Kuca K and Tobin G (2017) Acetylcholinesterase Inhibitors and Drugs Acting on Muscarinic Receptors- Potential Crosstalk of Cholinergic Mechanisms During Pharmacological Treatment. *Curr Neuropharmacol* **15**(4): 637-653.

Sykes DA, Dowling MR and Charlton SJ (2009) Exploring the mechanism of agonist efficacy: a relationship between efficacy and agonist dissociation rate at the muscarinic M3 receptor. *Mol Pharmacol* **76**(3): 543-551.

Tewson P, Westenberg M, Zhao Y, Campbell RE, Quinn AM and Hughes TE (2012) Simultaneous detection of Ca²⁺ and diacylglycerol signaling in living cells. *PLoS One* **7**(8): e42791.

Tewson PH, Martinka S, Shaner NC, Hughes TE and Quinn AM (2016) New DAG and cAMP Sensors Optimized for Live-Cell Assays in Automated Laboratories. *J Biomol Screen* **21**(3): 298-305.

MOL #109678

Tewson PH, Quinn AM and Hughes TE (2013) A multiplexed fluorescent assay for independent second-messenger systems: decoding GPCR activation in living cells. *J Biomol Screen* **18**(7): 797-806.

Thal DM, Sun B, Feng D, Nawaratne V, Leach K, Felder CC, Bures MG, Evans DA, Weis WI, Bachhawat P, Kobilka TS, Sexton PM, Kobilka BK and Christopoulos A (2016) Crystal structures of the M1 and M4 muscarinic acetylcholine receptors. *Nature* **531**(7594): 335-340.

Violin JD and Lefkowitz RJ (2007) Beta-arrestin-biased ligands at seven-transmembrane receptors. *Trends Pharmacol Sci* **28**(8): 416-422.

Weng L, Davies M and Ashcroft SJ (1993) Effects of cholinergic agonists on diacylglycerol and intracellular calcium levels in pancreatic beta-cells. *Cell Signal* **5**(6): 777-786.

Wess J (2004) Muscarinic acetylcholine receptor knockout mice: novel phenotypes and clinical implications. *Annu Rev Pharmacol Toxicol* **44**: 423-450.

Wisler JW, DeWire SM, Whalen EJ, Violin JD, Drake MT, Ahn S, Shenoy SK and Lefkowitz RJ (2007) A unique mechanism of beta-blocker action: carvedilol stimulates beta-arrestin signaling. *Proc Natl Acad Sci U S A* **104**(42): 16657-16662.

Wu G, Bogatkevich GS, Mukhin YV, Benovic JL, Hildebrandt JD and Lanier SM (2000) Identification of Gbetagamma binding sites in the third intracellular loop of the M(3)-muscarinic receptor and their role in receptor regulation. *J Biol Chem* **275**(12): 9026-9034.

Wuttke A, Yu Q and Tengholm A (2016) Autocrine Signaling Underlies Fast Repetitive Plasma Membrane Translocation of Conventional and Novel Protein Kinase C Isoforms in beta Cells. *J Biol Chem* **291**(29): 14986-14995.

MOL #109678

Footnotes:

This work was supported by the National Institutes of Health Grants [RO1DK105427, RO1DK111538].

MOL #109678

Legends for Figures

Figure 1. Pilocarpine is a full agonist in the pupil constriction assay. Mouse eyes were treated *ex vivo* with the indicated drugs, and pupil diameter was analyzed as described in Materials and Methods. (A) Photographs of the eyes after 1 h incubation in 10 mM pilocarpine or 0.01 mM CCh. (B) Time-course of pupil constriction in the presence of 10 mM Pilo or 0.01 mM CCh. (C) Eyes were treated with indicated concentrations of pilocarpine, Oxo-M and CCh for 10 min. Data show average \pm SD from three independent experiments. Symbols on the X-axis denote estimated K_d values for pilocarpine (30 μ M), Oxo-M (50 μ M) and CCh (150 μ M) (from Sykes *et al.* 2009). (D) *In situ* RNA hybridization of mouse eye section was performed using RNAscope approach (see Materials and Methods); shown is a representative image. Distinct green fluorescent dots correspond to individual mRNA molecules.

Figure 2. Pilocarpine acts as a cholinergic antagonist for endogenous M3R in HEK293T and MIN6 cells. Cells were grown on glass coverslips, loaded with fura-2, AM and imaged in a flow cell mounted under a fluorescence microscope. They were challenged with CCh and pilocarpine solutions, and fura-2 fluorescence was monitored in real time as described under Materials and Methods. (A) Dose-response curve for intracellular free Ca^{2+} in HEK293T cells in the presence of indicated concentrations of CCh or pilocarpine. The data points show mean peak response \pm SD, n=3. (B) Pilocarpine (Pilo, 300 μ M) was co-applied together with 25 μ M CCh, which resulted in blockade of calcium increase. After a 5 min wash with HBSS, the cells were challenged with 25 μ M

MOL #109678

CCh. The trace shows an average of 3 experiments recording fura-2 fluorescence from 40-60 cells. (C) MIN6 cells were challenged first with 300 μM pilocarpine, then with 100 μM Oxo-M, and free Ca^{2+} was recorded as in (B). (D) Insulin release from cultured MIN6 cells was determined by ELISA as described under Materials and Methods; cells were challenged with 100 μM Oxo-M, 500 μM pilocarpine or their mixture. Data are shown as the amount of insulin released to the medium compared to unstimulated cells (control; 1 $\mu\text{g/ml}$). Data show mean \pm SD, $n=3$, $p<0,01$.

Figure 3. Pilocarpine stimulates free Ca^{2+} mobilization in cells overexpressing M3R.

CHO-K1 or HEK293T cells were transiently transfected with M3R, M1R and fluorescent proteins. (A) Schematic of the experiment. Cells transfected to express M1R with eYFP or M3R with mCherry (red and green) are mixed and plated on coverslips. They are subsequently loaded with fura-2, AM and analyzed for sensitivity to cholinergic stimulation. (B, C) A representative image (200x magnification) of the mixed cell population. Red cells are co-transfected with plasmids encoding M3R and mCherry, green cells express eYFP together with M1R. The (C) panel illustrates selection of the regions of interest to collect data on Ca^{2+} . The blue traces denote cells that do not express fluorescent proteins and are visualized by fura-2 staining alone. See Materials and Methods for more detail. (D) Free Ca^{2+} responses to 10 μM pilocarpine and 10 μM CCh. Traces represent the average of responses recorded from 20-30 individual cells/regions of interest. The green trace corresponds to the data from M1R-expressing cells, red shows M3R, and black shows untransfected cells. Data shown are representative of at least three such experiments done with independent transfections. (E) Amplitude of Ca^{2+} responses

MOL #109678

was measured at the indicated concentrations of CCh or pilocarpine. (F) Experiment on HEK293T cells performed essentially as the one done on CHO-K1 cells (A-D). Note that there is a response of un-transfected cells to CCh, but not to pilocarpine. Representative of two independent transfection experiments.

Figure 4. Effect of pilocarpine on PIP2 hydrolysis. Cells were co-transfected with the PIP2 red biosensor and with the plasmids encoding M1R or M3R. Fluorescence was recorded in real time after cells stimulation with pilocarpine (Pilo) or CCh. (A) Representative images of CHO-K1 cells co-transfected with plasmids to overexpress M3R and the PIP2 sensor. The cells were grown on coverslips and imaged under fluorescence microscope in a flow chamber. (B) Traces show the average of fluorescence response from 20-30 HEK293T cells; red trace is response of M1R-expressing cells, green trace - M3R expressing cells, black - cells expressing only the PIP2 biosensor. Cells were challenged with the flow of solutions of 100 μ M Pilo or CCh at the indicated times. (C) PIP2 responses from CHO-K1 cells transfected with M1R (red) or M3R (green). Cells were stimulated with 100 μ M pilocarpine, Oxo-M or CCh. (D) PIP2 sensor fluorescence recorded from M3R-overexpressing HEK293 cells first challenged with 25 μ M CCh in the presence of 300 μ M pilocarpine (red and black horizontal bars), then washed and stimulated again with 25 μ M CCh (black bar). (E) Ca^{2+} responses from HEK293 cells expressing M3R (green) or control plasmid (black). Cells were stimulated with the mixture of pilocarpine and CCh or CCh alone as in (D).

MOL #109678

Figure 5. Ca²⁺ assay is more sensitive to agonist stimulation than PIP2 assay. CHO-K1 cells were transiently transfected with M1R- or M3R-encoding plasmids and analyzed for pilocarpine and CCh-stimulated Ca²⁺ increase and PIP2 hydrolysis. (A) M1R transfected cells were stimulated with indicated concentrations of CCh (black lines) or pilocarpine (red). Live cell imaging of free Ca²⁺ (solid lines) or PIP2 responses (dashed lines) was performed as described in Materials and Methods. Data points denote the maximal amplitude of the response and expressed at the % of the maximal response (mean±SD); N=3 or more. (B) CHO-K1 cells were transfected to overexpress M3R and analyzed like in (A). (C) CHO-K1 cells were transfected with M3R, stimulated with 1 μM pilocarpine in the absence of extracellular Ca²⁺ and analyzed for their Ca²⁺ response. Data shown are representative of at least three such experiments done with independent transfections.

Figure 6. Pilocarpine - stimulated Ca²⁺ and PIP2 signaling via endogenous and overexpressed M3R in HEK293 cells. HEK293 cells were transfected to overexpress M3R (red) or a control plasmid (lacZ, green), plated on glass coverslips and stimulated with indicated concentrations of CCh. Ca²⁺ (solid line, filled circles) or PIP2 (dashed line, empty triangles) were measured in real time using a fluorescence microscope. Data points represent peak amplitude (mean±SD, n=3) measured as average from 20-40 cells in a visual field.

Figure 7. Oxotremorine and cevimeline do not induce PIP2 hydrolysis via overexpressed M3R. (A) CHO-K1 cells were transfected to overexpress M3R and the

MOL #109678

PIP2 reporter, plated on glass coverslips and stimulated with 100 μ M of the indicated drugs. PIP2 responses (green lines) were measured in real time using a fluorescence microscope. The traces show an average of 3 experiments recording fluorescence from 20-30 cells for each compound. ACh – acetylcholine, Pilo – pilocarpine, Oxo – oxotremorine. (B) Structures of the tested muscarinic agonists.

Figure 8. Pilocarpine stimulates ERK1/2 phosphorylation in MIN6 cells via a PP2-sensitive pathway. (A) MIN6 cells were serum-starved for 4 h and then stimulated for 5 min with the indicated concentrations of Oxo-M or pilocarpine (Pilo). The amount of phosphorylated ERK1/2 was determined by western blot using anti-P-ERK1/2(T202/Y204) antibody. The same membrane was also stained with an anti-actin antibody used for signal normalization. Shown is a representative immunoblot. (B) Quantification of ERK1/2 phosphorylation in response to stimulation with Oxo-M (blue) or pilocarpine (Pilo, red) was done as described in Materials and Methods. Data show mean \pm S.D. from three independent experiments. (C) PP2, a Src family kinase blocker, inhibits pilocarpine- and Oxo-M-stimulated ERK1/2 phosphorylation. MIN6 cells were serum-starved and pre-incubated with the indicated concentrations of PP2 for 4 h. Then they were stimulated for 5 min with either 1 μ M Oxo-M (blue) or 100 μ M pilocarpine (Pilo, red). ERK1/2 phosphorylation was determined as in A and B. Shown is a representative immunoblot and data quantification (mean \pm S.D. from three independent experiments). (D) A PKC inhibitor bisindolylmaleimide I (BIM, 10 μ M) almost completely blocks Oxo-M-stimulated ERK1/2 phosphorylation when combined with PP2

MOL #109678

(60 μ M). The experiment was performed and quantified as in C. Data show mean \pm S.D. from three independent experiments.

Figure 9. A proposed model for CCh and pilocarpine action via M3R. When either CCh (or other agonists such as acetylcholine and Oxo-M) or pilocarpine (Pilo) bind to M3R, the receptor assumes two similar but distinct conformations. The CCh-bound M3R is able activate Gq, leading to stimulation of PLC β and subsequent signaling cascade steps. It also activates β -arrestin-mediated signaling cascade, leading to stimulation of ERK1/2. In contrast, the pilocarpine-bound M3R conformation is unfavorable for Gq activation. In fact, by competing with CCh, pilocarpine can antagonize the Gq-dependent signaling cascade. However, pilocarpine is still able to activate β -arrestin-dependent signaling that leads to ERK1/2 phosphorylation.

MOL #109678

Table 1. Analysis of Ca²⁺ and PIP2 responses to CCh and pilocarpine in M1R and M3R-expressing cells. CHO-K1 or HEK293T cells were transfected with either M1R or M3R-expressing plasmids. Non-transfected HEK293 cells were used to study the endogenous M3R present in these cells. The EC₅₀ and Emax were determined for pilocarpine (Pilo) and CCh in two functional assays, free Ca²⁺ and PIP2 measurements. The experiments were performed as discussed in the text and Materials and Methods. Shown are means ± S.D. for the values determined in 3-4 independent experiments. n.a. – not applicable; n.d – not determined; the “-” sign indicates that no functional response was detected under these conditions.

		CHO-K1				HEK293T			
		Ca ²⁺		PIP2		Ca ²⁺		PIP2	
		EC50, μM	Emax, %	EC50, μM	Emax, %	EC50, μM	Emax, %	EC50, μM	Emax, %
endogenous M3R	Pilo	n.a.	n.a.	n.a.	n.a.	-	0	-	0
	CCh	n.a.	n.a.	n.a.	n.a.	11±2	44±5	-	0
transfected M3R	Pilo	0.19±0.06	71±6	-	0	n.d.	n.d.	-	0
	CCh	0.06±0.02	100	4±1	100	0.04±0.01	100	4±1	100
transfected M1R	Pilo	0.21±0.07	84±7	2±0.6	83±8	n.d.	n.d.	n.d.	n.d.
	CCh	0.11±0.04	100	1.2±0.4	100	n.d.	n.d.	n.d.	n.d.

Figure 1

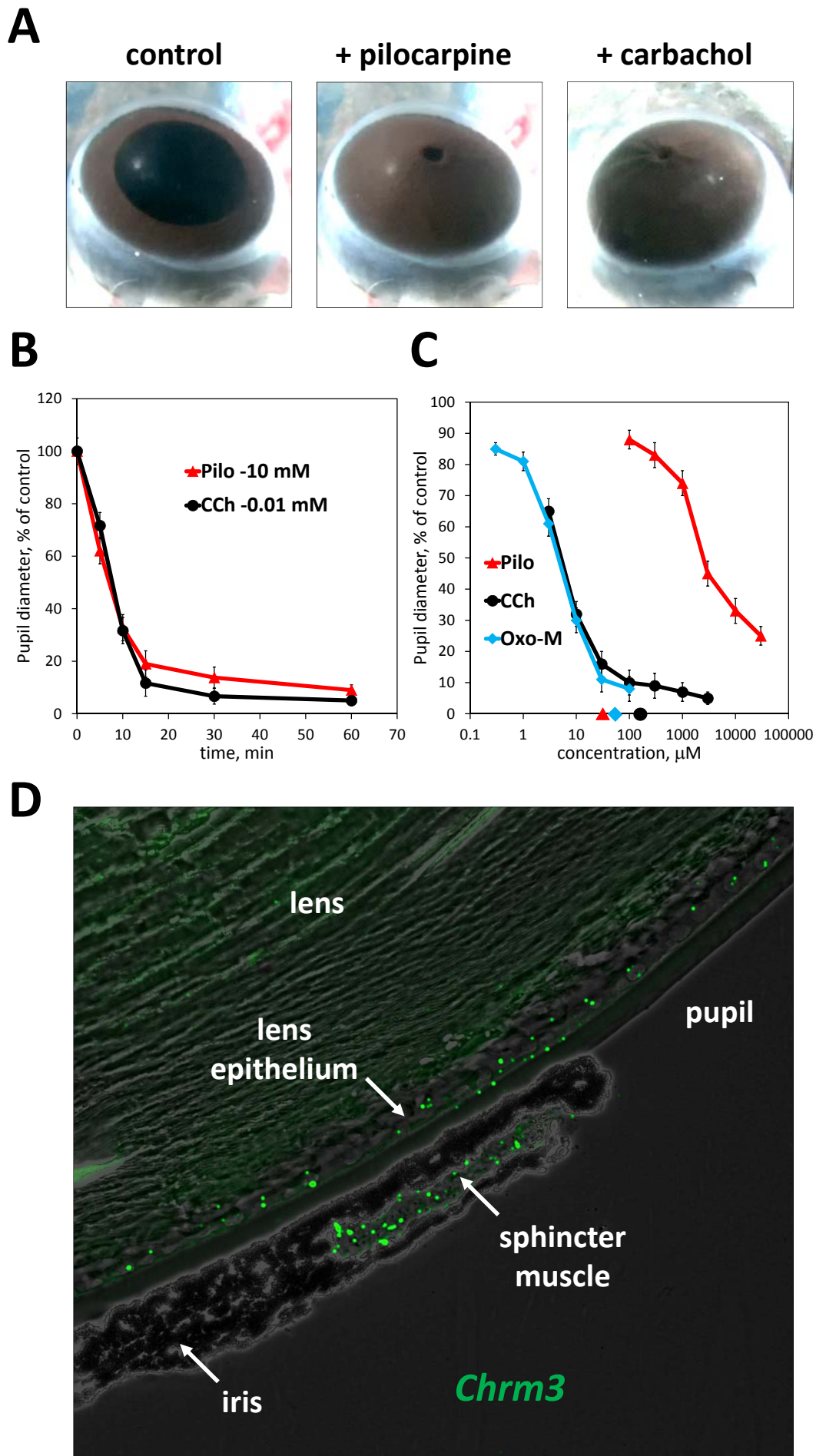


Figure 2

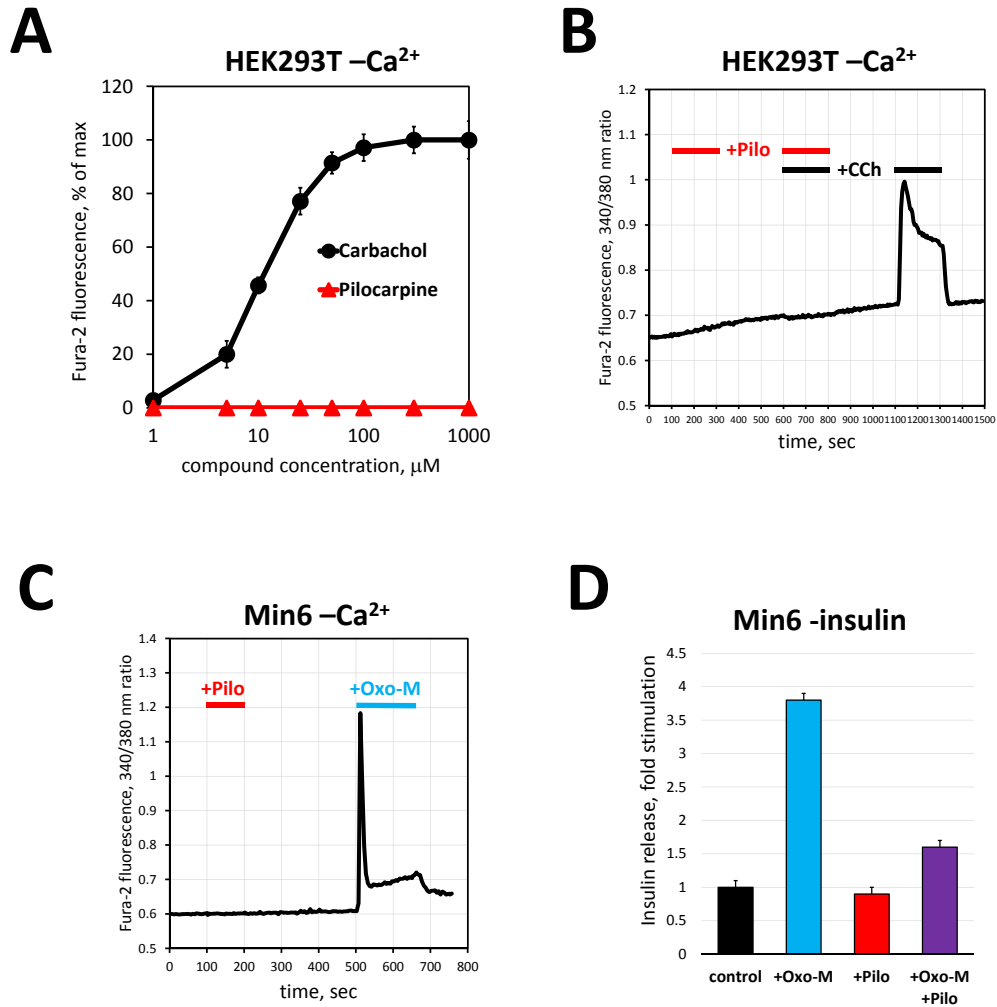


Figure 3

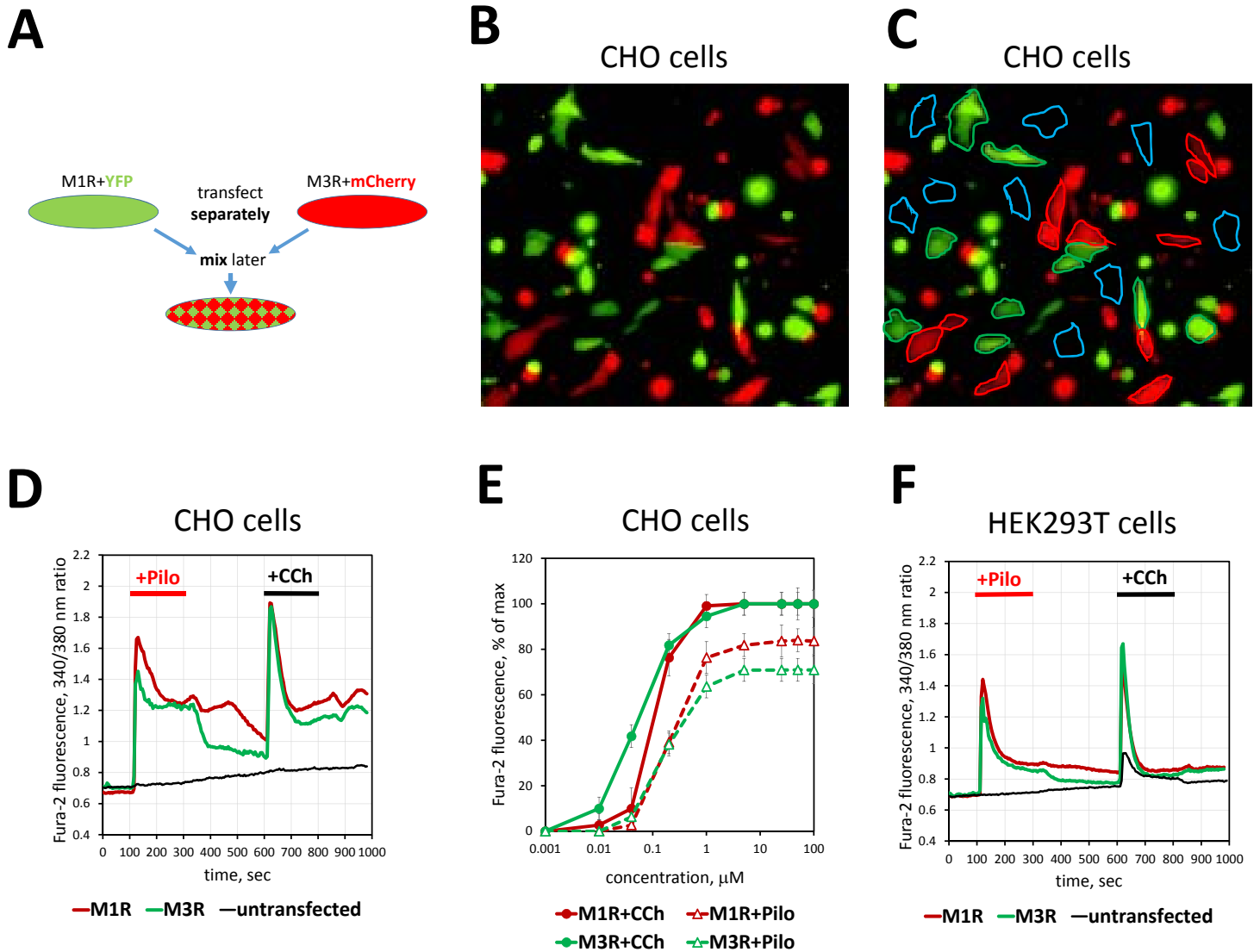
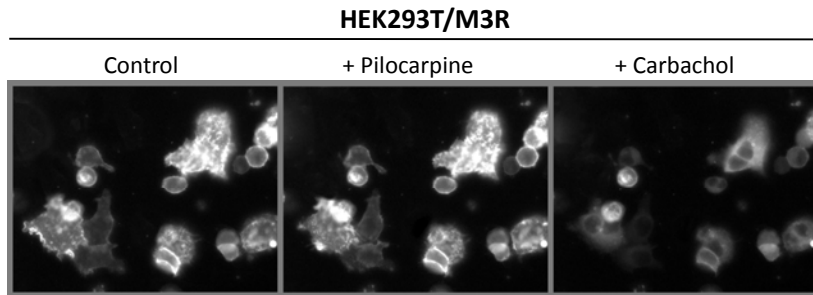
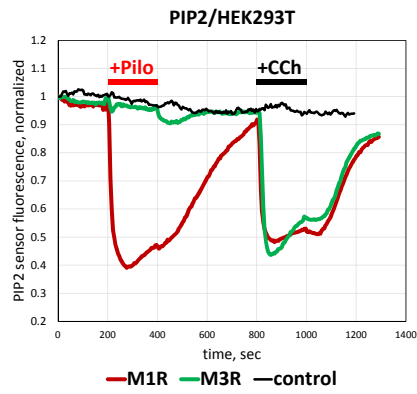


Figure 4

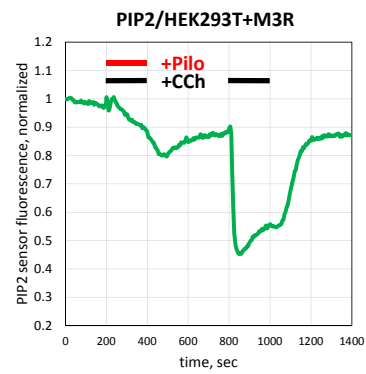
A



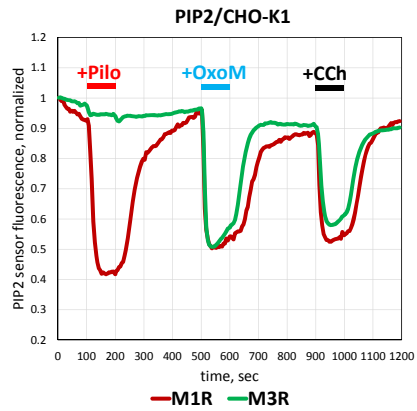
B



D



C



E

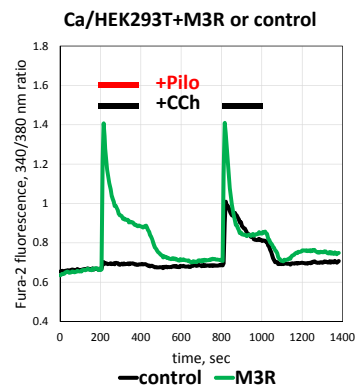


Figure 5

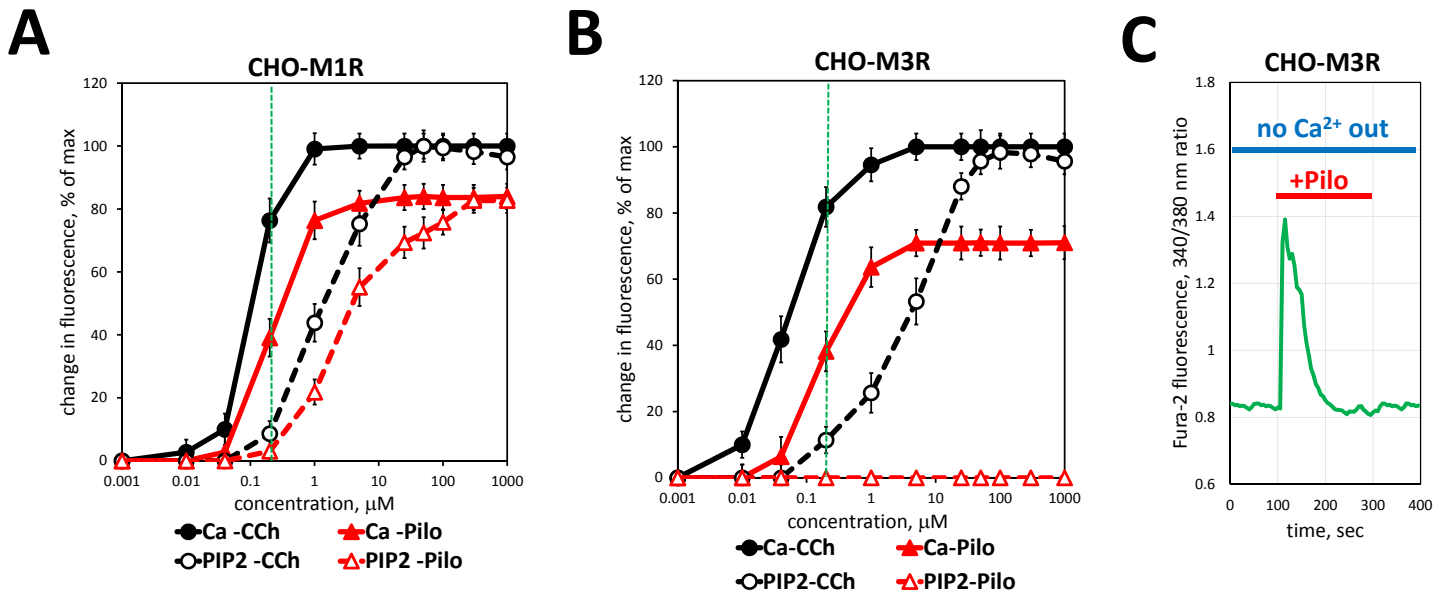


Figure 6

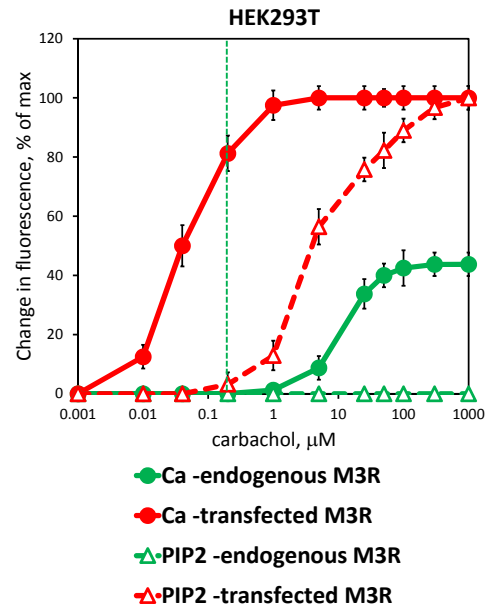


Figure 7

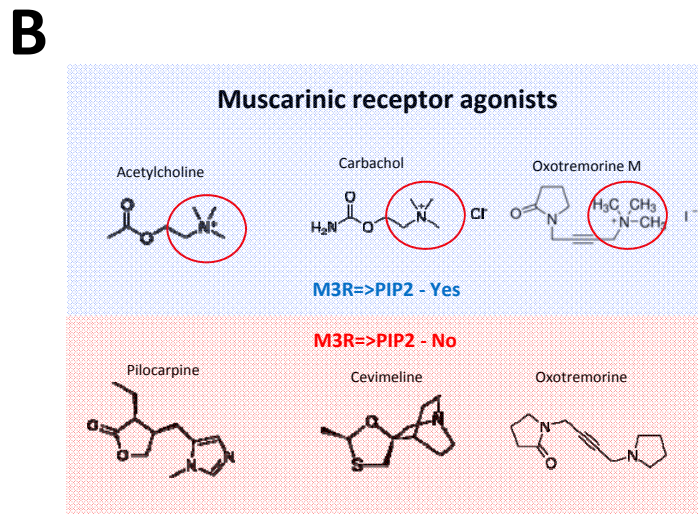
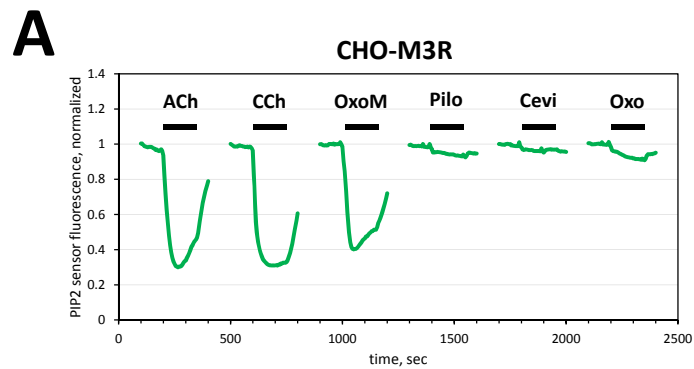


Figure 8

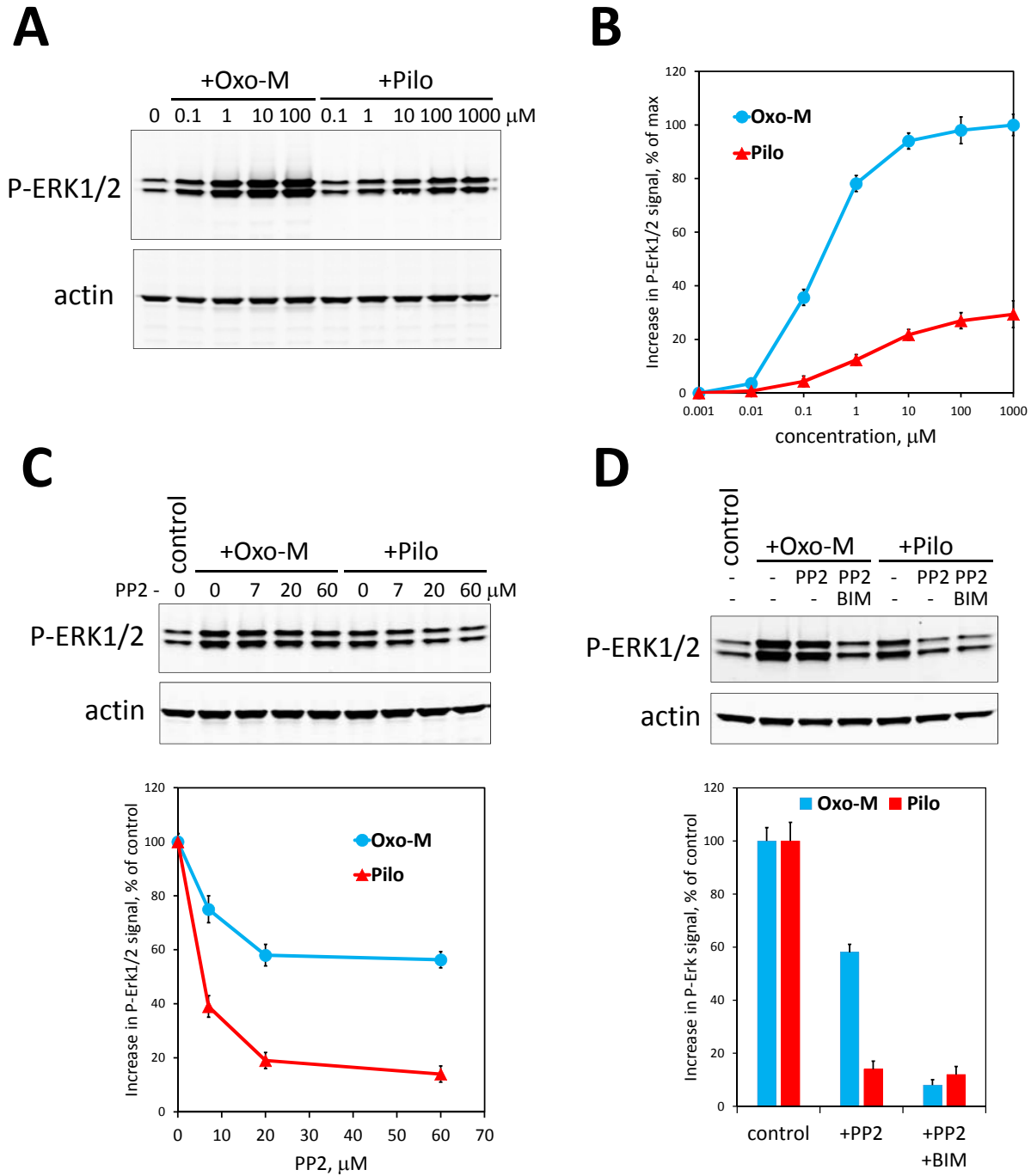


Figure 9

